NOTAE PRAEHISTORICAE 45

45ste Prehistoriedag
45ème Journée de Préhistoire
45. Tag der Ur- und Frühgeschichte
Gent - 12.12.2025

FNRS Contactgroep
« Prehistorie »
Groupe de Contact FNRS
« Préhistoire »
Kontaktgruppe FNRS
« Ur- und Frühgeschichte»

Organisation

Isabelle De Groote
Hans Vandendriessche, Philippe Crombé
Universiteit Gent, Vakgroep Archeologie
35, Sint-Pietersnieuwstraat, BE-9000 Gent
www.Archeos-UGent.be – www.roam-ugent.be

with the collaboration of / avec la collaboration de / met medewerking van

Coordination scientifique / Wetenschappelijke coördinatie / Wissenschaftliche Koordination

Jean-Philippe Collin
Philippe Crombé
Marc De Bie
Isabelle De Groote
Anne Hauzeur
Ivan Jadin
Stéphane Pirson
Veerle Rots
Bart Vanmontfort
Philip Van Peer

Another site of the Swifterbant Culture in the Lower Scheldt valley: finds from A600 Scheldetunnel Linkeroever (Antwerp, BE)

Dimitri Teetaert, Daan Celis, Frédéric Cruz, Samuel Bodé, Lucy Kubiak-Martens, Koen Deforce, Coralie André, Elliot Van Maldegem, Lies Dierckx, Veerle Hendriks, Femke Martens & Philippe Crombé

1. Introduction

In Antwerp, the construction of a third Scheldt crossing was initiated in 2018. This major infrastructure construction project is intended to complete the Antwerp ring road. The development is referred to as the Oosterweel Link, named after the polder village of Oosterweel, which has almost completely disappeared due to the expansion of the port of Antwerp. At Linkeroever, a neighbourhood situated on the left bank of the Scheldt, the tunnel emerges near Sint-Annabos. The project directly impacts both the remains of the American repatriation camp "Top Hat", established during the Second World War, as well as older stratigraphic horizons extending into prehistoric periods. Camp Top Hat was investigated archaeologically in the spring of 2021, while excavations targeting the prehistoric landscape were carried out in the spring of 2023 (**Fig. 1**).
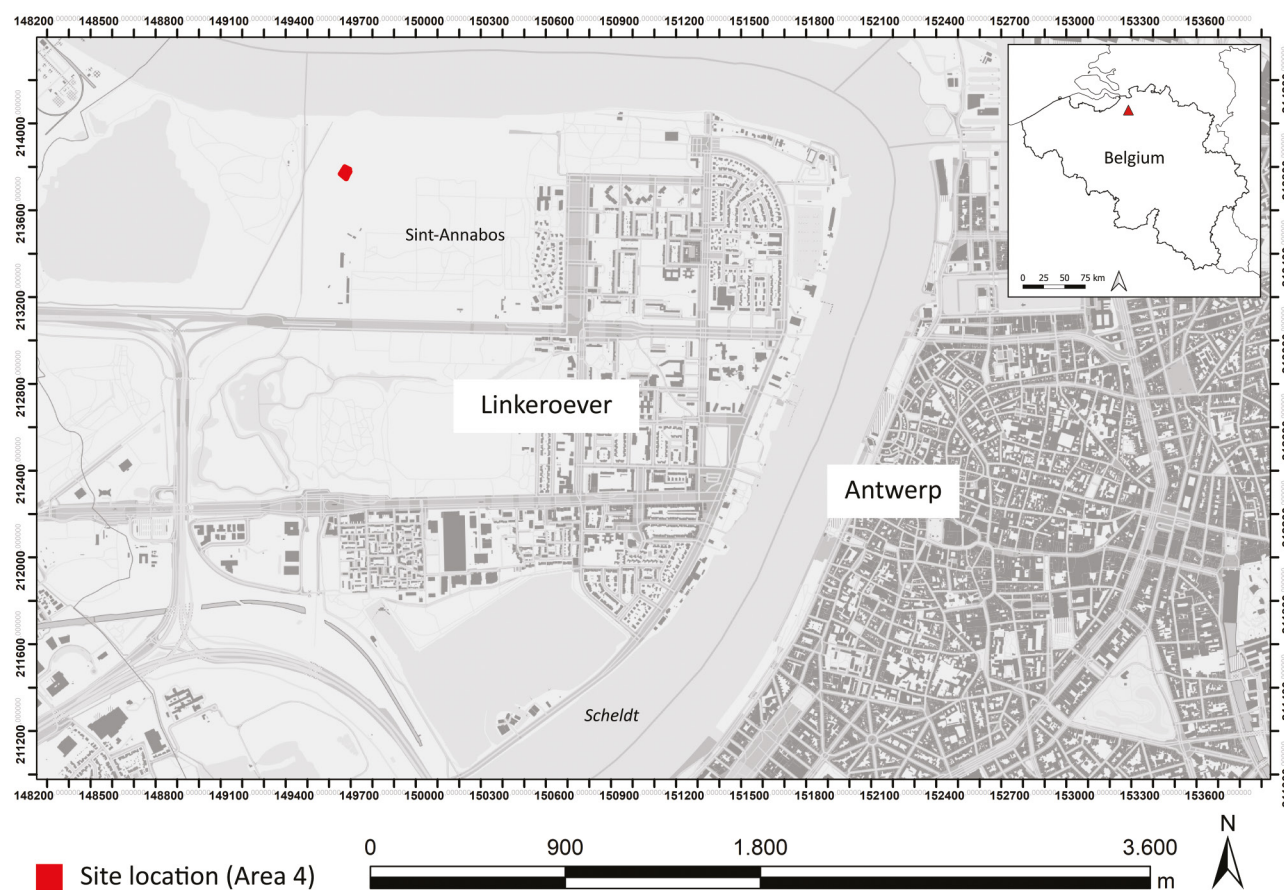

Fig. 1 – Location of site A600 Scheldetunnel Linkeroever – Area 4 (51°14′04.3″N, 4°21′50.2″E).
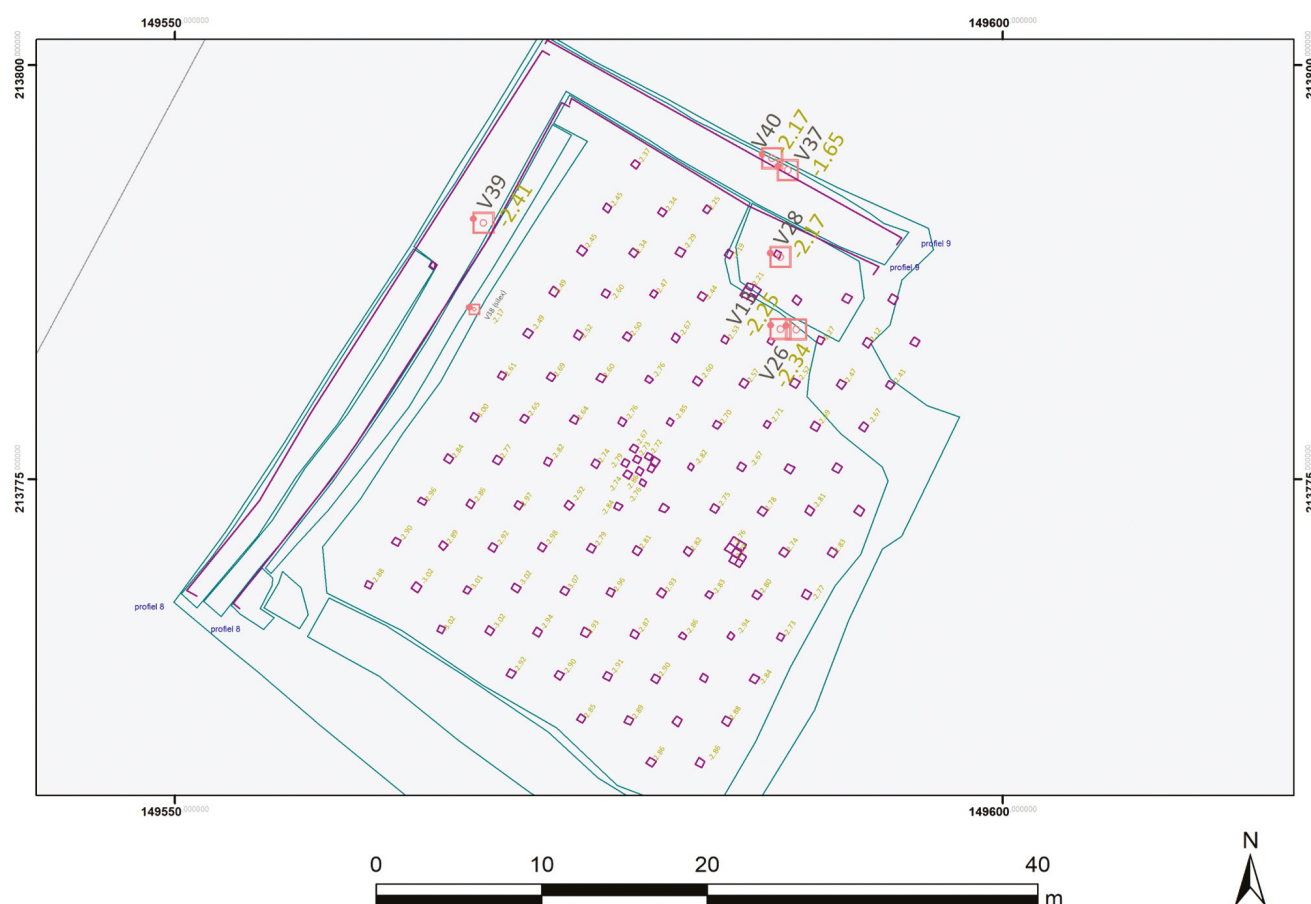
Fig. 2 – Map of Area 4 with indication of the test pits and find locations of the prehistoric artefacts.

Preliminary archaeological research was carried out, starting with an extensive desktop research combined with a programme of landscape coring. Coring following a 10 x 10 m grid revealed an undisturbed peat horizon overlying a Pleistocene substratum. An exploratory coring campaign, comprising 585 samples, yielded a single flint flake of possible anthropogenic origin (Vansweevelt, 2020). This evidence was regarded too tenuous to warrant further investigations of the prehistoric levels, such as further coring.

Instead, test pits on a 3 x 2 m grid (each measuring 0.50 x 0.50 m) were excavated within a 30 x 30 m area centred on the positive core, in order to investigate the extent of the prehistoric "site" (**Fig. 2**). Sediments extracted from the test pits were wet-sieved using a 2 mm mesh in search for lithic artefacts and ecofacts. Aside from a single artefact, *i.e.* the proximal fragment of a bladelet, the 115 test pits all proved negative for the presence of flint artefacts. However, archaeological material was found around the excavation of these test pits and through the registration of landscape sections, predominantly at the interface between the peat and the underlying Pleistocene substratum.

These material finds, consisting of five fragments of handmade pottery and two antler artefacts, are the focus of this paper. The pottery and antler artefacts were subjected to typo-technological analysis, and for the pottery this was complemented by residue analysis. In addition, four radiocarbon dates were obtained on the antler artefacts, the food residue, and the peat adhering to one of the potsherds. Finally, two subsamples of this peat were analysed palynologically. Based on these analyses, it is suggested that the pottery and antler fragments are related to a nearby settlement of the Swifterbant Culture, dating around the middle to the third quarter of the 5th millennium cal BCE.
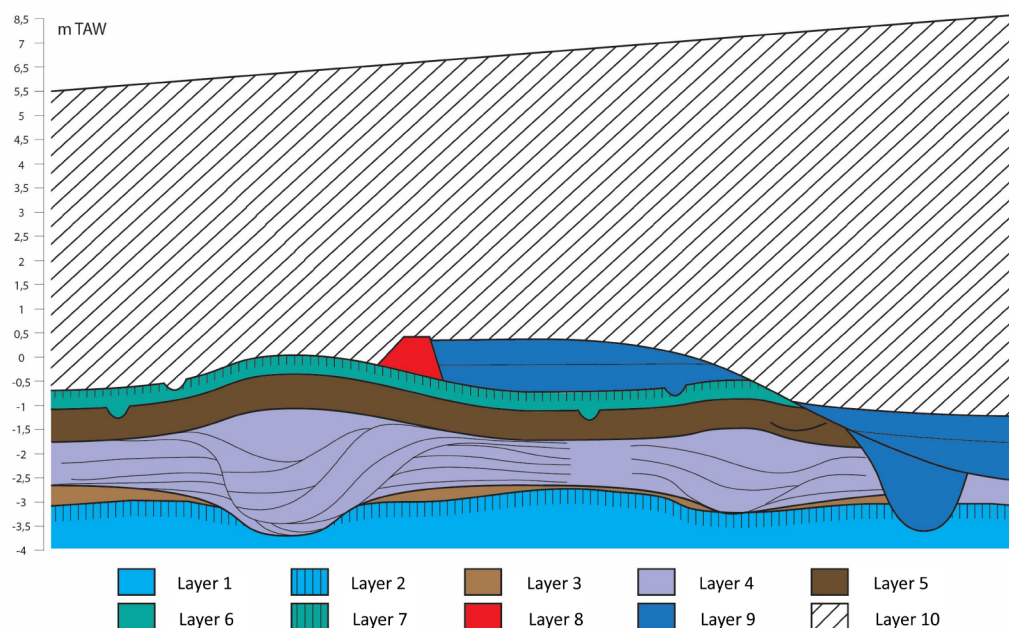
Fig. 3 – Schematic representation of the site stratigraphy. 1: Weicheslian alluvium; 2: pedogenesis upon alluvium; 3: subsoil peat; 4: estuarine environment; 5: topsoil peat; 6: intertidal sediment; 7: pedogenesis upon intertidal sediment; 8: dykes; 9: dyke breach; 10: anthropogenic embankment. TAW = mean low water tide level in Ostend, West Flanders, Belgium.

2. Site and stratigraphy

A total of 12 landscape profile trenches were excavated within the project area of the first tunnel section. Ten distinct stratigraphic phases were documented across all trenches (**Fig. 3**), spanning a period from prehistory up to the 20th century levelling with sand dredged from the Scheldt. The earliest phase is marked by stratified sands deposited by a river during the Weichselian glacial period (Fig. 3, layer 1). At the top of this sequence, a 10 cm thick A-horizon developed as a result of pedogenesis (Fig. 3, layer 2). With climate amelioration starting in the Late Glacial, sedimentary stability was established and arboreal vegetation expanded. Abundant traces of bioturbation were identified within this palaeosol, including faunal burrows and roots from collapsed or uprooted trees. Erosion channels and small gullies reflect localised fluvial reworking along micro-slopes, probably linked to anthropogenic disturbance such as deforestation, clearance of undergrowth, or episodic forest fires.

During subsequent phases, increasingly humid climatic conditions accelerated the accumulation of peat to several decimetres thick (Fig. 3, layer 3). Around a small local gully, eroded within this peat, trampling traces were observed, suggesting that the water feature functioned as a watering place for both animals and humans.

The prehistoric finds reported in this paper, including both ceramic and antler artefacts (**Tab. 1**), were recovered at the first centimetres of the base of this peat horizon, at the contact zone between layers 2 and 3, in Area 4 and in profile trenches 8 and 9 (Cruz & Rozek, 2023). Notably, the highest concentration of finds occurred in the northeastern sector of the excavation area, where slightly elevated micro-topography provided seasonally drier, and thus more accessible conditions in the Holocene wetland environment. Since no prehistoric finds were collected above the basal peat, the higher stratigraphic levels will not be further discussed in this paper.

Find number	Material	Depth
V13	Antler mattock	-2.25 m TAW
V26	Ceramic body sherd	-2.34 m TAW
V28	Antler production waste	-2.17 m TAW
V37	Ceramic base	-1.65 m TAW
V39	Ceramic body sherd	-2.41 m TAW
V40	Ceramic body sherd	-2.17 m TAW

Tab. 1 – List of prehistoric finds from site A600 Scheldetunnel Linkeroever with their position in relation to the sea level (TAW).

Fig. 4 – Round base with transition to the lower vessel body (V37). The arrow indicates the location of an external Z join.

3. Pottery

The excavations in Area 4 of site A600 Scheldetunnel Linkeroever yielded a small assemblage of handmade pottery, consisting of four body sherds (V26, V39 & V40) and one base (V37). The pottery remains were retrieved from the contact zone between the Pleistocene coversand and the covering peat layer. The base was found upright, with peat encrusted to its inner surface.

3.1. Typo-technological analysis

The round base is *ca*. 8 cm in diameter and 22 mm thick (**Fig. 4**). Its fabric consists of a silty to slightly sandy clay, rich in iron oxides. The latter are well visible at the vessel surfaces (**Fig. 5A**) and represent natural inclusions in the clay. The pottery clay is heavily tempered with grog. In addition, several fine, rectilinear voids at the vessel surfaces indicate the presence of fine plant material, that was either naturally present in the clay or added as temper. The lower body of this vessel, partly preserved in attachment to the base, is built by an external overlap of clay coils. This is indicated by the diagonal orientation of the clay mass in radial section (so-called "Z" configurations) and the presence of an external Z join (Fig. 4). The forming of the base itself is less clear, but it seems to have been either modelled from a lump of clay or built by spiral coiling.

The four body sherds have a similar fabric of silty to slightly sandy clay, with a limited amount of iron oxides and grog temper (**Fig. 5B**). They probably do not belong to the same vessel as the round base, which is richer in iron oxides and grog fragments, yet the similarities in the fabrics indicate that all of this pottery belongs to the same occupation phase. The largest body sherd (**Fig. 6**) is 11 mm thick and likely to be situated at the lower body or lower to upper body transition. Based on the presence of circular ("O") to subcircular ("C") clay configurations in radial section, in combination with a U join, the body of this vessel was built by the superposition of non- or only slightly deformed coils (*cf*. Livingstone Smith, 2001; Gomart, 2014). Both the inner and outer surface of this vessel have been burnished, as indicated by the lustrous surfaces with burnishing facets. The other three body sherds also show signs of burnishing, but they are too small to provide further technological information.

3.2. Lipid analysis

3.2.1. Materials and methods

To gain better insight into the use of these vessels, pottery powder was sampled from the base (V37) and largest body sherd (V26) for lipid analysis, including molecular analysis by gas chromatography-mass spectrometry (GC-MS) and isotopic analysis by gas chromatography-combustion-isotope ratio mass spectrometry (GC-C-IRMS). For this
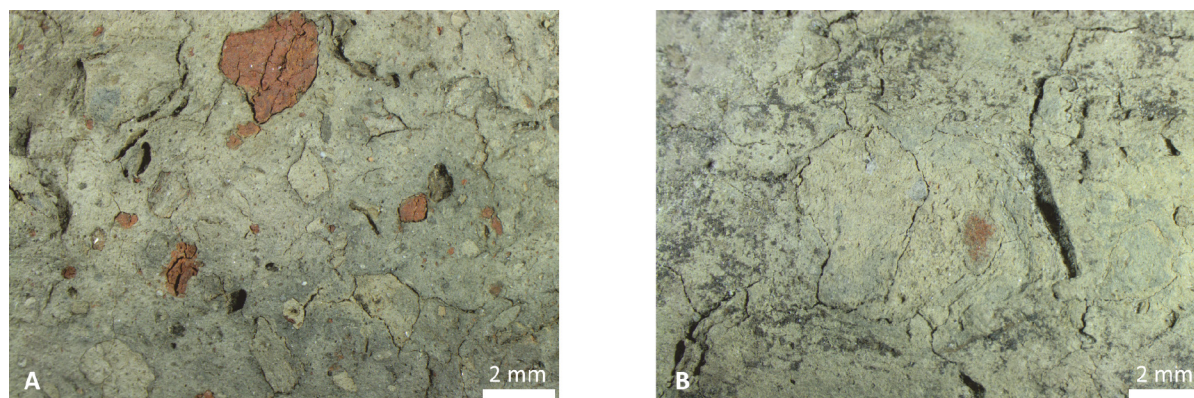
Fig. 5 – Detail of the fabrics of the base (A) and largest body sherd (B) using a Olympus SZX7 stereo microscope.

purpose, *ca*. 1 g of pottery powder was extracted from the internal part of both potsherds, after removal of the pottery surface to reduce the risk of contamination, using a power tool with a miniature tungsten carbide tip (Dremel). In addition, the same analyses were performed for the food crusts adhered to the inner surface of the largest body sherd.

After initial sampling, the pottery powder and food crusts were extracted using the one-step acidified methanol protocols (Correa-Ascencio & Evershed, 2014; Papakosta *et al.*, 2015). In short, *ca*. 1 g of pottery powder (or 0.1 g of food crust) was transferred to a reaction vial together with 10 µg *n*-tetratriacontane recovery standard dissolved in Hexane (1 mg/mL) together with 4 (or 1) mL HPLC grade methanol. After short vortexing 800 (or 200) µL 99 % H_2SO_4 was added cautiously, sealed with a PTFE lined cap, vortexed again and heated for 4 h at 70 °C. The lipid fraction was extracted from the acidified methanol using three times 2 mL of hexane. A small scoop of Cu turnings were added to the extract to remove sulphur, and more Cu was added if needed (visible by the blackening of the Cu turnings). Finally, 10 µg of *n*-hexatriacontane was also added to the extract as internal standard. Molecular composition of the extracts was determined using GC-MS (Trace GC, coupled to a ISQ-MS, Thermo Scientific). Separation was done using a DB-5 (30 m x 0.25 mm x 0.25 µm) column. Identification of molecules present in the extract was done using a combination of a targeted, and not targeted approach. The targeted molecules are listed in **table 2**, further all visible peaks in total ion current (TIC) and in chromatograms
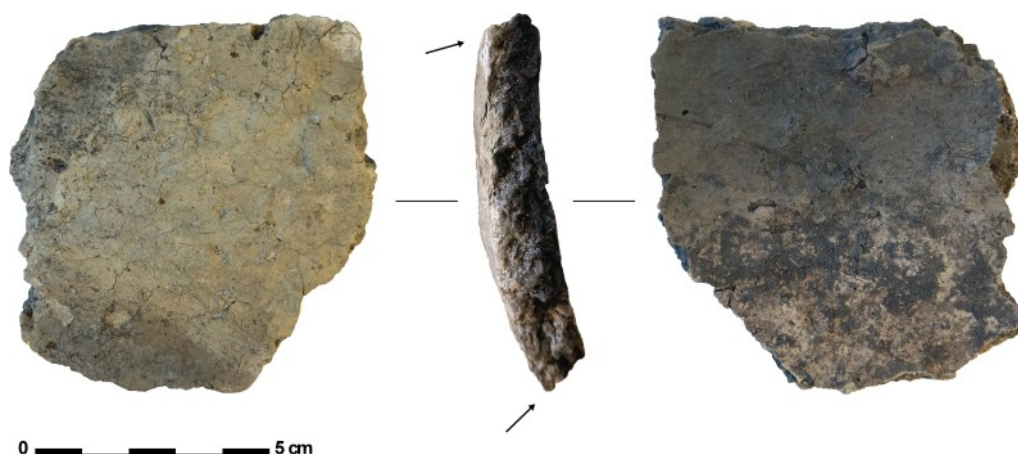

Fig. 6 – Surfaces and radial section of the largest body sherd (V26). The arrow indicates the location of a (reversed) U join. The picture to the right shows charred organic residue adhered to the inner surface.

Group	Compound	Sample OW01	OW02	OW03
Straight saturated FA	12:0	NF	1.36	1.14
	14:0	NF	3.09	3.21
	15:0	1.29	1.85	2.18
	16:0	195.78	32.76	43.38
	17:0	19.86	1.46	1.38
	18:0	348.17	32.59	32.23
	19:0	3.67	0.50	0.37
	20:0	8.88	1.69	2.22
	21:0	1.28	0.39	0.42
	22:0	7.85	1.56	2.12
	23:0	2.68	0.41	0.41
	24:0	8.84	1.08	1.79
	25:0	1.58	0.19	0.31
	26:0	4.23	0.53	0.89
	27:0	0.73	0.07	0.12
	28:0	3.20	0.35	0.56
	30:0	2.25	0.19	0.31
Branched FA	i15:0	NF	0.23	0.21
	a15:0	NF	0.32	0.33
	i16:0	0.60	0.45	0.45
	i17:0	3.18	0.27	0.33
	a17:0	2.83	0.40	0.46
	i15:0	NF	0.23	0.21
	Squalene	86.41	10.47	11.93
Unsaturated FA	16:1	1.23	1.11	0.79
	18:1	16.17	0.96	0.56
	18:2	NF	NF	NF
	18:2	NF	NF	NF
	22:1	13.16	7.02	5.89
Der. from PUFA	APAAs (from 18:3)	NQ	NQ	NF
	APAAs (from 20:3)	NF	NF	NF
	Pristanic acid	NF	NF	NF
	Phytanic	NF	NF	NF
	TMTD	NF	NF	NF
Alkanes	C21	1.40	0.27	0.27
	C27	8.11	0.20	0.59
	C29	49.85	0.47	1.89
Dicarboxylic acids	Dicarb. 8:0	0.02	0.13	0.23
	Dicarb. 10:0	NF	NF	NF
	Dicarb. 11:0	NF	NF	NF
	Dicarb. 12:0	NF	NF	NF
Plastic contamination	Dimethyl_Phtalate	NF	0.47	0.40
	Phthalic_acid_ester_(plasticiser)	1074.17	18.36	16.93

Tab. 2 – Semiquantitative overview of the molecular identification of the lipid extract (µg/g).
Samples: OW01 = food crusts from body sherd (V26);
OW02 = pottery powder from body sherd (V26);
OW03 = pottery powder from base (V37).
NF: No peak could be identified at the expected retention time, nor in TIC nor in SIM.NQ: peak was to low for proper quantification and confident identification.

of most relevant m/z were also identified (**Fig. 7**). Semi-quantification was done assuming an identical response factor for the TIC peak area of analytes and the internal standard. When a specific ion current was used, a correction for the area of the specific ions and TIC on well separated peaks of the compound of interest or similar compounds was used.

Compound specific stable isotope (CSSI) analysis of palmitic and stearic methylated fatty acid was analysed using GC-IRMS (GC 1310 – GC-ISOLINK – ConFLo IV – Delta V, all Thermo scientific) after adaptation of the volume of hexane. Normalization was done using the F8-4 methyl/ethyl ester mixture from Arndt Shimmelman injected every two to three sample injections, matching sample concentration. All samples were analysed at least in duplicate, differences on $\delta^{13}C$ were always smaller than 0.2 ‰. After analysis the obtained data for the fatty acid methyl esters was corrected for the added methyl group.

To identify the origin of the extracted fatty acids, the $\delta^{13}C$ values of the palmitic (C16:0) and stearic (C18:0) fatty acid methyl esters (FAMEs) obtained from the samples were compared to those of modern authentic reference animals (after correction for the Suess Effect). A dataset of $\delta^{13}C$ values for modern authentic reference animals fed with a paleo diet, as published by Courel *et al.* (2020), was used as dietary endmember signature. This reference data has been broadly grouped into five potential food sources (freshwater, marine, porcine, ruminant adipose, ruminant dairy). Furthermore, the difference in $\delta^{13}C$ values between stearic and palmitic fatty acid ($\Delta 13C$) is considered a robust criterion for separation between non-ruminant adipose fats ($\Delta 13C$ > ca. -2 ‰), ruminant adipose fats ($\Delta 13C$ between *ca.* -1 and -5 ‰) and ruminant dairy fats ($\Delta 13C$ < -3.1 ‰) (Copley *et al.*, 2003; Craig *et al.*, 2012; Cramp & Evershed, 2014).

3.2.2. Results

The molecular analysis (GC-MS) reveals a similar pattern for all three samples, with a clear dominance of palmitic (16:0) and stearic (18:0) acid (**Fig. 7**), followed by two peaks that most likely represent post-excavation contamination, *i.e.* phthalic acid ester (plasticiser) and squalene. Most saturated, straight fatty acids from 12:0 till 30:0 are positively identified in all samples (Tab. 2).

The 16:0 and 18:0 content of all three samples was sufficient for compound specific $\delta^{13}C$ analysis of the palmitic and stearic acids by GC-C-IRMS. When comparing the obtained $\delta^{13}C$ values with those reported by Courel *et al.* (2020), all samples fall within a region of overlap between the reference ranges for freshwater and ruminant adipose fats (**Fig. 8**). Therefore, both freshwater resources (e.g. fish) and ruminant meat/fat could have been processed in these vessels.
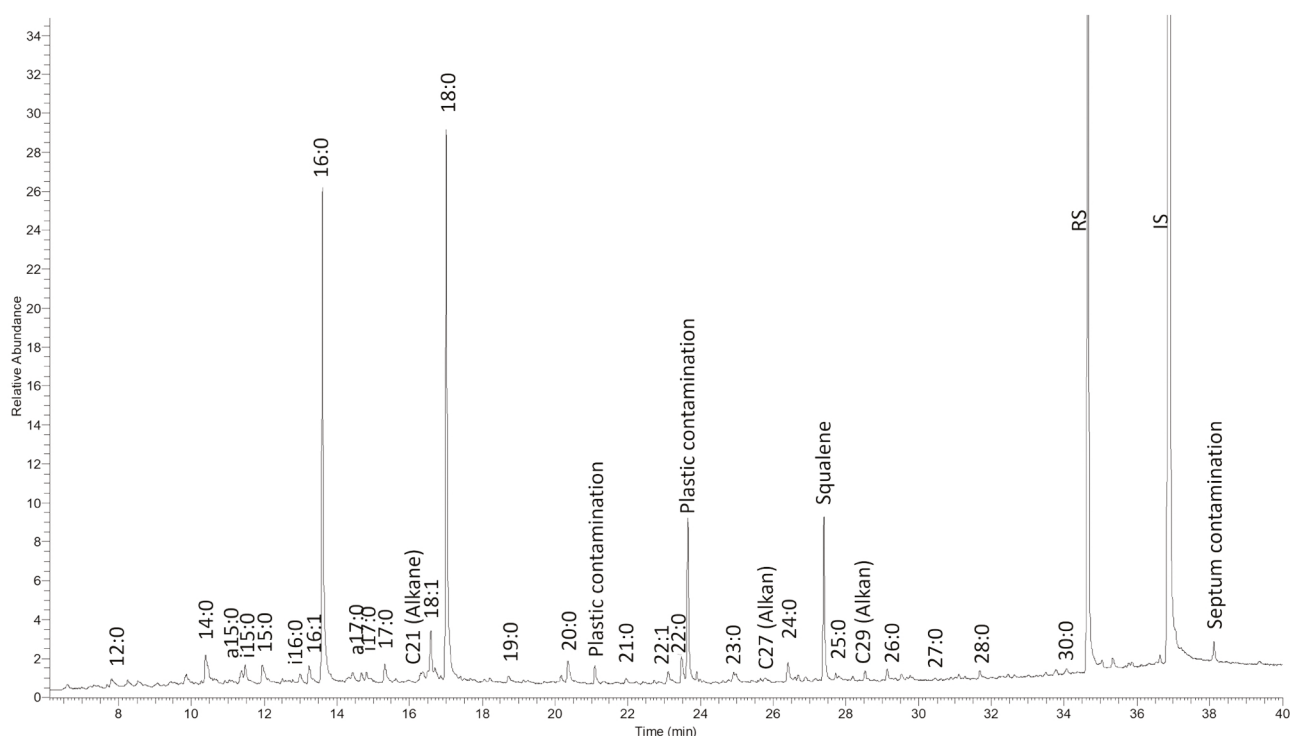
Fig. 7 – Partial GC-MS chromatogram of the total ion current (TIC) of a representative sample (OW02 = pottery powder from body sherd V26) with positive identified peaks. RS and IS denote the recovery and internal standard, respectively.

Clear biomarkers for freshwater resources are however missing from the molecular data. For instance, isoprenoid acids (pristanic, phytanic and 4,8,12-trimethyltridecanoic acid (TMTD)), particularly recalcitrant indicators of aquatic fats (Copley *et al.*, 2004; Regert, 2011; Casanova *et al.*, 2022), were not detected in any of the samples. The presence of *ω*-(o-alkylphenyl)alkanoic acids (APAAs) derived from C18:3, 20:3 and 22:3 is also considered as indicative of the processing (heating to > 200°C) of aquatic fats (Hansel *et al.*, 2004; Cramp & Evershed, 2014; Bondetti *et al.*, 2020). Although a small peak close to the expected retention times of one of the C18:3 derived APAA isomers was noted in the chromatograms of two out of three samples, its abundance was too low for a positive identification.

The mono-unsaturated fatty acids C16:1, C18:1 and C22:1 were positively identified in all samples (Fig. 7, Tab. 2), although they were present in very low abundances. These compounds are sometimes related to aquatic fats but are also found in terrestrial animal fats, plant oils and soil microorganisms. On the other hand, mono-branched fatty acids of C15:0 and 17:0 are abundant in ruminant adipose fats (Evershed *et al.*, 1997; Demirci, 2022). These compounds were positively identified (i15:0, a15:0, i17:0 and a17:0; Fig. 7; Tab. 2), but again their abundance is low and they also widely occur in other lipid sources (including soil microorganisms) and should therefore be interpreted with caution (Demirci, 2022).

The palmitic/stearic acid ratios (P/S ratios) might provide more information. Although palmitic and stearic acids are present in both animal and plant sources, stearic acid is generally found in higher concentration in terrestrial animals than aquatic and plant food sources (Craig *et al.*, 2007; Papakosta *et al.*, 2015; Demirci *et al.*, 2020). In the studied samples, the P/S ratios are situated between 0.95 and 1.37. In the literature, P/S ratios < 2 have been considered as indicative of terrestrial animal lipids (Papakosta *et al.*, 2015), although ruminant adipose fats are generally considered to have P/S ratios < 1 (Romanus *et al.*, 2007; Regert, 2011; Baeten *et al.*, 2013). Freshwater fish (and plant oils), however, have P/S ratios typically > 3 (Craig, 2004).
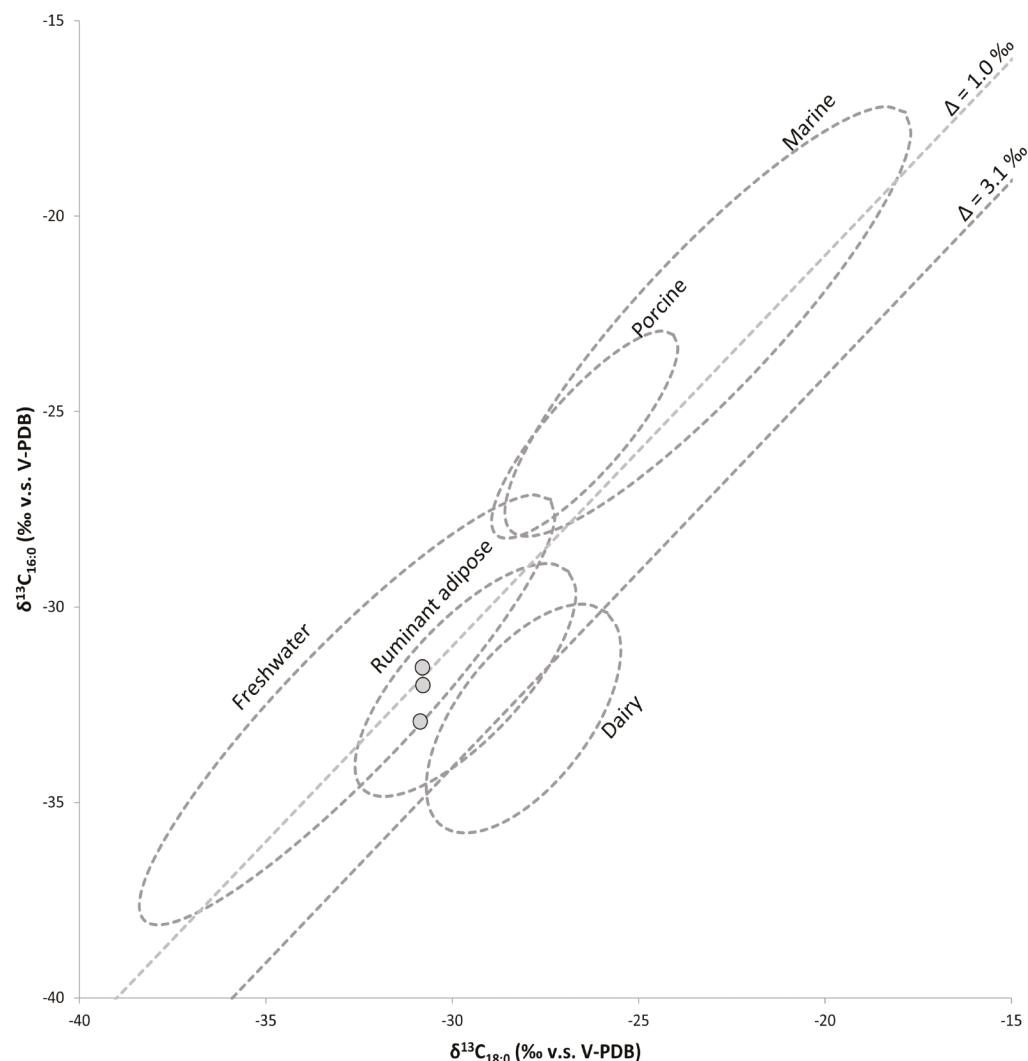
Fig. 8 – δ¹³C values of C16:0 and C18:0 fatty acids from the pottery powder and food crust samples. 95 % confidence ellipses indicate the range of δ¹³C16:0 and δ¹³C18:0 values from modern authentic reference animals, corrected for the Suess Effect (Courel *et al.*, 2020). The diagonal lines represent Δ13C values of -1 and -3.1 ‰, often used as a cut-off for ruminant adipose fats and dairy fats respectively.

Finally, three straight alkanes (C21, C27 & C29) could be identified in all samples. Long chain off numbered alkanes are typically considered as indicative of the presence of plant derived lipids, and the predominance of C27 and C29 points toward a woody plant origin (Bush & McInerney, 2013). Also the presence of long (> C20) and short chain (< C16) fatty acids gives some indication of the presence of plant derived lipids (Dunne, 2022).

To conclude, the combined lipid analyses indicate that these vessels were used for cooking. Based on the GC-C-IRMS results, both freshwater resources and ruminant meat/fat might have been processed in these vessels. The P/S ratios rather point towards the processing of ruminant meat/fat. However, although clear biomarkers for aquatic products are missing from the molecular data, their presence should not be ruled out. Finally, although plant lipids are often difficult to detect in pottery, especially when mixed with animal fats (Steele *et al.*, 2010; Craig *et al.*, 2020), the molecular data indicate that plant components were processed in these vessels as well.

3.3. SEM analysis

3.3.1. Materials and methods

Food crusts are preserved on the inner surface of the largest body sherd (Fig. 6). These crusts were analysed by Scanning Electron Microscopy (SEM) to study the residue's microstructure and provide information on any food components that have been preserved inside this residue. For the SEM analysis, nine fragments of residue were selected, to ensure maximum coverage and account for potential variations in the composition within the crust/cooking/heating event. Selected portions of residues were mounted on the SEM stubs using carbon cement. The samples were sputter-coated with a thin layer of platinum-palladium, approximately 20 µm thick. The analysis was carried out at the Naturalis Biodiversity Center in Leiden, using a JEOL JSM-6480L scanning electron microscope.

3.3.2. Results

The residue matrix does not contain any recognisable plant particles, animal bone or fish scales. However, numerous thread-like structures or 'microwires' with a hollow inner section were observed, embedded in an otherwise featureless matrix (**Fig. 9**). These hollow tubes, resembling microtubules, are remarkably fine, measuring 3-4 µm in diameter. They were preserved as isolated fragments (Fig. 9, top) or clustered together and branching out (Fig. 9, below).
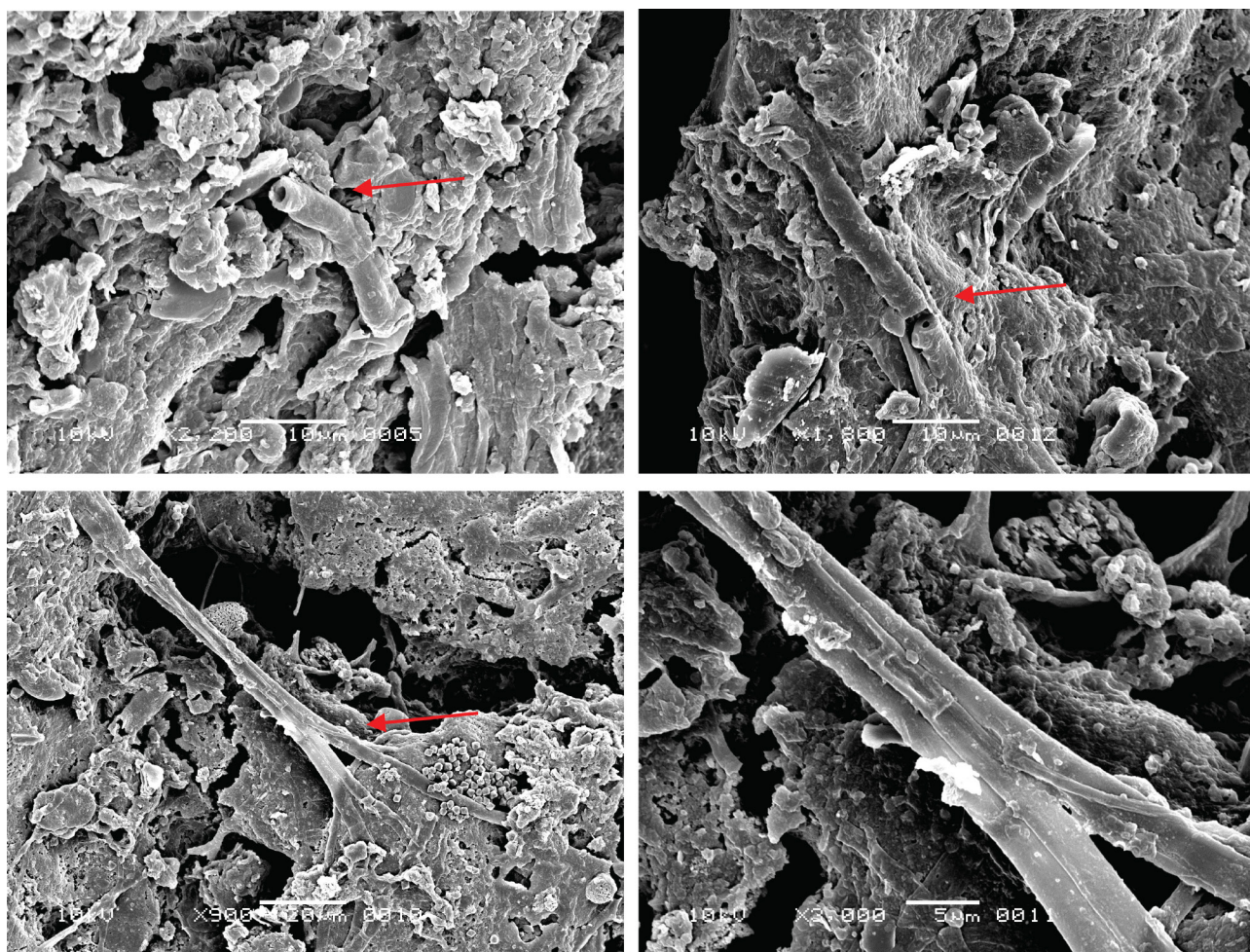

Fig. 9 – SEM images showing the internal microstructure of the organic residue. The red arrows indicate thread-like structures or 'microwires' with a hollow inner section (resembling microtubules) embedded in an otherwise featureless matrix. Images by L. Kubiak-Martens, Biax Consult.

The determination of the nature of these thread-like structures within the residue matrix is challenging. Several possibilities, such as aimal hair, rootlets, or sponge spicules, can be ruled out based on the dimensions or morphological characteristics of these structures. Currently, the only suggested identification is that they are fungal hyphen. The dimensions of microtubules in fungi can vary among different species, but generally, they are quite small, from 2-8 μm to up to several millimetres in length (Fontes *et al.*, 2014; Kubo *et al.*, 2016), which corresponds with the dimensions of the observed features.

The potential presence of fungi might indicate that a fermentation process was involved in the preparation of food, e.g. to be able to store the fermented products for a longer time (see Craig, 2021). However, we should also consider the possibility that food remains inside the vessel moulded unintentionally. Finally, fungal infiltration of the residue from the soil, as part of post-depositional processes, cannot be ruled out.

3.4. Interpretation

Due to the small number of sherds and the limited amount of diagnostic fragments, we must remain cautious in interpreting and culturally attributing this pottery. Nevertheless, there are clear technological and typological parallels with the pottery of the Swifterbant culture (5th millennium cal BCE) in the Lower Scheldt valley (Crombé, 2010; Teetaert, 2020; Teetaert & Crombé, 2022). Currently, only five sites of the Swifterbant culture are known in this region, all located within a radius of approximately 12 km around site A600 Scheldetunnel Linkeroever. These include the sites at Doel Deurganckdok (B, J and M), Melsele Hof ten Damme, and Bazel Sluis (van Berg *et al.*, 1992; Crombé, 2005; Crombé *et al.*, 2015a; Meylemans *et al.*, 2016). The Swifterbant pottery from these sites is primarily tempered with grog, sometimes in combination with fine plant material, more specifically mosses (Teetaert *et al.*, 2020). It is made from local Tertiary or alluvial clays, and pottery with fabrics rich in iron oxides are known from Doel site J and Melsele Hof ten Damme (Teetaert & Crombé, 2022). The fabric of the pottery from site A600 closely resembles this. Pottery from the Swifterbant sites is consistently constructed from clay coils and is, in most cases, smoothed. Although conical or pointed bases also occur, round bases are the most common. It appears that the pottery from site A600 can be placed within the same cultural context. The stratigraphic position in which the artefacts were found – on top of the Pleistocene coversand or in the contact zone between this sand and the covering peat – is also very similar (Deforce *et al.*, 2014; Crombé *et al.*, 2015b). Furthermore, the available radiocarbon dates seem to confirm this chrono-cultural interpretation (*cf.* infra).

4. Antler artefacts

4.1. Typo-technological analysis

- Fig. 10-A: Longitudinal fragment of a perforated mattock (V13) measuring 154 mm (length) x 43 mm (width) x min. 26 mm (thickness). One extremity has been modified into an oblique, polished cutting edge. It presents a rounded edge resulting from intense polishing. Parallel to the cutting edge an oval perforation (diameter 19 mm) was made. Clear cutting traces, up to 2 to 4 cm long, are preserved at both sides of the perforation. The extremity opposite the cutting edge is partly destroyed; however, a small part displaying a rounded edge indicates that the original mattock was probably not much longer. Typologically it corresponds either to Hurt type E or Hurt type C. The former type is a mattock made on a tine, while the latter is a mattock made on a section of the beam above the trez tine (Hurt, 1982).

- Fig. 10-B: Basal fragment of a shed red deer antler (V28) (diameter 59 mm) with preserved brow tine, the latter partially destroyed at its extremity. The main beam has been removed intentionally as indicated by the presence of two parallel and deep grooves running parallel to the burr across half the circumference. This resulted in an oblique fracturing of the main beam starting from just below the bez tine, the onset of which is still preserved.
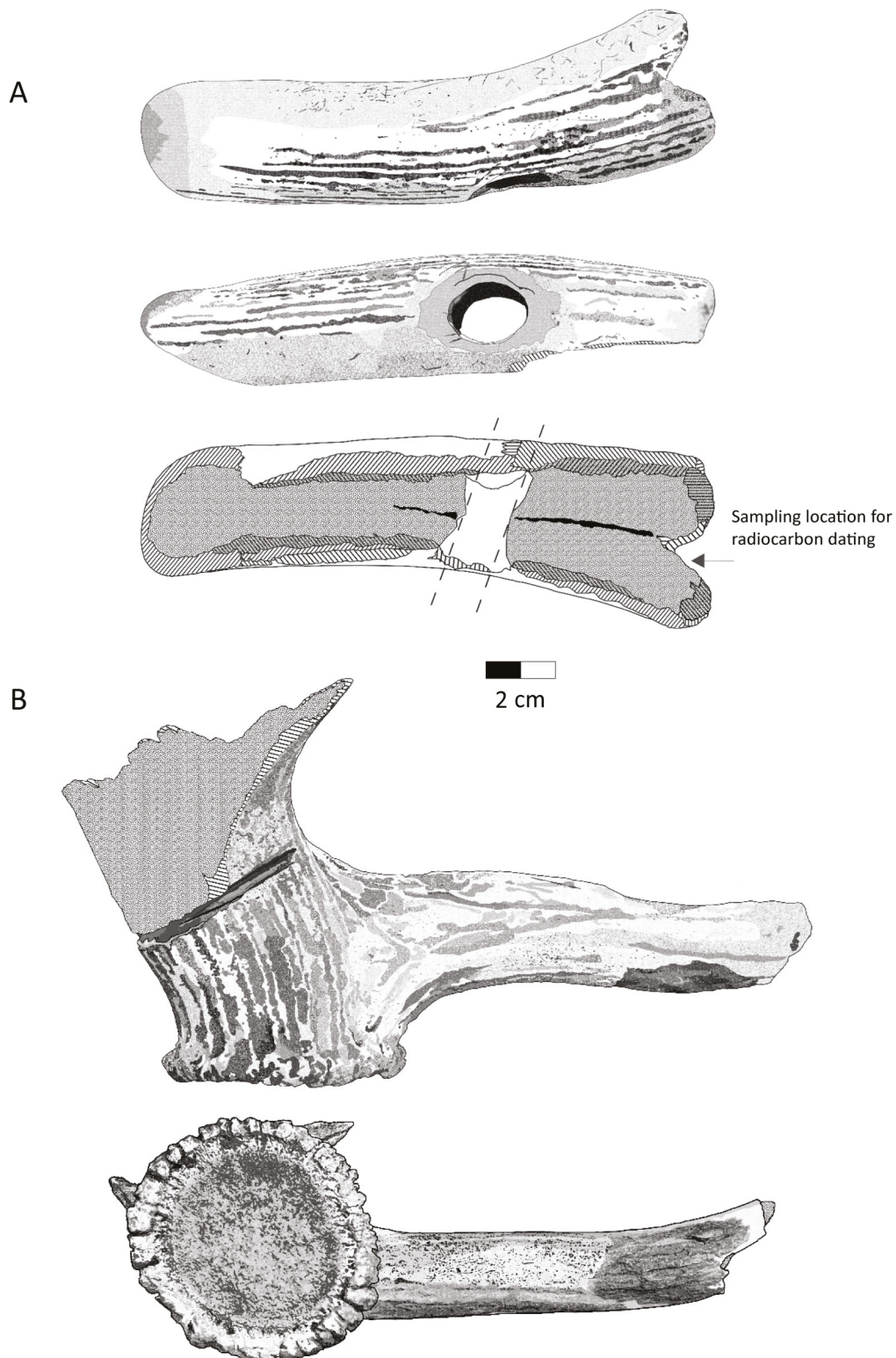
A

B

Sampling location for
radiocarbon dating

2 cm

Fig. 10 – A: Longitudinal fragment of a perforated mattock (V13); B: Basal fragment of red deer antler (V28).

4.2. Interpretation

Within the Scheldt valley Hurt type C and E antler mattocks seemingly occur less frequently compared to antler-base (type A) and T-shaped antler-beam mattocks (type B). However, this could be due to focused (radiocarbon) research on both the latter types (Hurt, 1982; Crombé *et al.*, 1999, 2018). Yet within the Dutch wetlands they generally also seem to be rather rare, except at the famous Swifterbant Culture site of Hardinxveld-Polderweg (Louwe Kooijmans *et al.*, 2001). Here, type I (beam mattocks) and type J (tine mattocks) frequently occur. However, these mattocks are rarely provided with a perforation.

The second antler fragment (V28) is clearly associated with the production of Hurt type B mattocks (T-shaped mattocks), typical of the 5th and first half of the 4th millennium cal BCE (Crombé *et al.*, 1999, 2018). It is totally excluded that it concerns waste from the production of the perforated mattock found on the site, since the latter does not display traces of a cut-off bez tine. Similar waste products have been found at different locations in the Scheldt valley, however never in stratigraphic position or in association with cultural remains, such as pottery.

5. Radiocarbon dates

Four radiocarbon dates were obtained at the ^{14}C laboratory of the Royal Institute for Cultural Heritage, following the standard procedures (Wojcieszak *et al.*, 2020; Boudin *et al.*, 2015, 2016-2018). Two of these dates were measured on the antler artefacts (**Tab. 3**). Both fall within the same chronological range and could statistically correspond to the same event, *ca*. 4454-4361 cal BCE [$\chi 2$, df = 1, T = 0.283 (5 % 3.841)]. This is contemporaneous with the earliest Swifterbant occupations at the nearby sites of Doel Deurganckdok (Messiaen *et al.*, 2022).

Two additional dates were obtained in order to date the pottery. One direct date was measured on food crusts adhering to the inner surface of the largest body sherd (V26), while a second, indirect date was obtained on peat attached to the interior of the base fragment (V37). The two results are not compatible, as indicated by a failed χ^2 test [df = 1, T = 7.093 (5 % 3.8)]; they differ by approximately 130 cal years.

The food crust date may have been affected by a reservoir effect resulting from the preparation of freshwater fish in the vessel. Although GC-MS analysis did not reveal clear aquatic biomarkers in the studied pottery, isotopic analysis by GC-C-IRMS indicates the possible presence of freshwater resources. Previous residue analyses of Swifterbant Culture pottery from the Lower Scheldt valley have shown that these vessels were frequently used to process freshwater fish (Teetaert *et al.*, 2024). Moreover, nearly all radiocarbon dates obtained on food crusts from this pottery (*n* = 47) show a reservoir effect, *i.e.* these dates are systematically up to several hundred years older than those obtained on organic macro-remains (e.g. charred seeds) from the same sites (Boudin *et al.*, 2009, 2010; Teetaert *et al.*, 2017).

Sample	Lab code	BP date	Calibrated date range (95.4 % probability)	% C	% N	δ13C (‰ v.s. V-PDB)	δ15N (‰ v.s. AIR)	C:N
Antler mattock (V13)	RICH-34792	5580±26	4448-4362 BCE	39.7	14.4	-22.2	2.6	3.2
Antler base fragment (V28)	RICH-34793	5607±25	4488-4365 BCE	42.9	15.4	-23.1	4.9	3.2
Peat attached to pottery (V37)	RICH-34755	5648±30	4537-4447 BCE					
Food crust on pottery (V26)	RICH-34791	5761±30	4679-4547 BCE					

Tab. 3 – List of radiocarbon dates. AMS ^{14}C determinations were modelled in Oxcal version 4.4.4 (Bronk Ramsey, 2009) using the IntCal20 atmospheric calibration curve (Reimer *et al.*, 2020).

The peat date provides a *terminus ante quem* for the pottery, since the peat formed after the deposition of the potsherds in the soil. However, the reliability of this date remains uncertain. Because the peat date was obtained on a bulk sample, a reservoir effect caused by the presence of aquatic plants cannot be fully excluded.

Hence, it remains difficult to assess whether the antler artefacts and pottery from site A600 Scheldetunnel Linkeroever are perfectly contemporaneous and represent a single event. It is also possible that they belong to different occupation events at the same location, around the middle to the third quarter of the 5th millennium cal BCE.

6. Palynological analysis

Two subsamples of the peaty sediment that was still attached to the inside of the base fragment were analysed for pollen and other palynomorphs to provide information on the environmental setting of the occupation that produced the pottery fragments. The two samples (*ca*. 2 ml each) were processed following standard procedures for pollen analysis (Moore *et al.*, 1991). Both showed a very low concentration of pollen grains which were also poorly preserved, with many pollen grains showing an exine that was damaged by corrosion. Only one of the subsamples, the one with a slightly higher pollen concentration has been analysed (**Tab. 4**).

The results reflect a local environment dominated by alder (*Alnus,* ~45 %) and ferns (*Filicales*, ~66 %), indicating the presence of an alder carr. This is confirmed by numerous scalariform perforation plates (~25 %) and spores of the fungus *Brachysporium* (~56 %), both indicators of decaying wood (Shumilovskikh *et al.*, 2015). Oak (*Quercus*), lime (*Tilia*) and hazel (*Corylus*) were likely growing on a higher part of the sand ridge or other sand ridges in the area.

The high percentage of chlamydospores of the arbuscular fungus *Glomus* (~53 %) and the presence of a pollen grain of *Carya* both indicate soil erosion. As there are no indications for tidal activity or sediment brought in by alluvial dynamics, the high *Glomus* percentages likely result from soil disturbance on the higher part of the sand ridge. The spores of the fungus *Diporotheca* (~22 %), which are also indicative of disturbed and eroded soils, such as those resulting from trampling (Hillbrand *et al.*, 2012), further corroborate this hypothesis.

In contrast to many other sites in the lower Scheldt valley where middle Holocene peaty sediments show indications for estuarine influence, often contemporaneous with the Swifterbant occupations, (Deforce, 2014; Crombé *et al.*, 2015b; Storme *et al.*, 2020), this is not the case in this sample. The low percentages of Chenopodiaceae and absence of other potential halophytes and marine microfossils exclude any marine influence and the low

Residue number	ArP 505	
Species	*n*	Fraction of
Trees and shrubs	152	96.2 %
Alnus	71	44.9 %
Betula	2	1.3 %
Carya	1	0.6 %
Corylus avellana	13	8.2 %
Fraxinus excelsior	1	0.6 %
Pinus sylvestris	17	10.8 %
Quercus	24	15.2 %
Salix	4	2.5 %
Tilia	18	11.4 %
Ulmus	1	0.6 %
Herbs	6	3.8 %
Chenopodiaceae	2	1.3 %
Cyperaceae	3	1.9 %
Potentilla type	1	0.6 %
Pollen sum	158	100.0 %

Aquatic plants		
Sparganium type	1	0.6 %
Spore plants		
Filicales	104	65.8 %
Polypodium vulgare	2	1.3 %
Pteridium aquilinum	10	6.3 %
Sphagnum	3	1.9 %
Algae		
Type HdV-210 (*Spirogyra* spore)	2	1.3 %
Type HdV-61 (*Mougeotia* zygospore)	1	0.6 %
Plant remains		
Type HdV-114 (scalariform perforation plate)	40	25.3 %
Fungi		
Type HdV-44 (*Ustulina deusta* ascospore)	17	10.8 %
Type HdV-121 (ascospore)	1	0.6 %
Type HdV-140 (*Valsaria variospora* ascospore)	1	0.6 %
Type HdV-143 (*Diporotheca* ascospore)	35	22.2 %
Type HdV-207 (*Glomus* chlamydospore)	84	53.2 %
Type HdV-359 (*Brachysporium* spp. spore)	89	56.3 %
Other fungi	61	38.6 %
Other NPP's		
Type HdV-988 (unknown microfossil)	16	10.1 %

Indeterminate	15	9.5 %
Concentration (pollen grains per ml)	4500	

Tab. 4 – Results of the palynological analysis of a peat sample attached to the inside of the base fragment (V37). Results are expressed as percentages of the sum of trees, shrubs and herbs.

percentages of willow (*Salix,* < 3%) exclude freshwater tidal environments nearby (Storme *et al.*, 2020). The occurrence of the freshwater algae *Spirogyra* and *Mougeotia* on the other hand point to stagnant, shallow and mesotrophic freshwater at the site (van der Wiel, 1982). The poor pollen preservation in the studied sample suggests that the water level may have dropped below the surface at times.

7. Conclusions

Both the typo-technological characteristics and the radiocarbon dates indicate that the pottery and antler artefacts from site A600 Scheldetunnel Linkeroever fall within the cultural context and time span of the Swifterbant Culture in the Lower Scheldt valley, currently dated to approximately 4600-4000 cal BCE. These finds most likely originate from one or several nearby occupations dating to the middle to third quarter of the 5th millennium BCE, situated along the left bank of the Scheldt river. Its location in the landscape closely resembles that of the nearby Swifterbant (and multi-period) sites of Melsele-Hof ten Damme and Bazel Sluis, highlighting the considerable potential for discovering additional sealed Swifterbant Culture sites in this area, for instance in the context of expansions of the Port of Antwerp.

References

Baeten J., Jerbvis B., De Vos D. & Waelkens M., 2013. Molecular evidence for the mixing of Meat, Fish and Vegetables in Anglo-Saxon coarseware from Hamwic, UK. *Archaeometry*, 55(6): 1150-1174. https://doi.org/10.1111/j.1475-4754.2012.00731.x

Bondetti M., Scott E., Courel B., Lucquin A., Shoda S., Lundy J., Labra-Odde C., Drieu L. & Craig O. E., 2020. Investigating the formation and diagnostic value of ω-(o-alkylphenyl)alkanoic acids in ancient pottery. *Archaeometry*, 63(3): 594-608. https://doi.org/10.1111/arcm.12631

Boudin M., Van Strydonck M. & Crombé P., 2009. Radiocarbon dating of pottery food crusts: reservoir effect or not? The case of the Swifterbant pottery from Doel Deurganckdok (Belgium). In: Crombé P., Van Strydonck M., Boudin M., Sergant J. & Bats M. (ed.), *Chronology and evolution within the Mesolithic of North-West Europe*, Cambridge Scholars Publishing, Newcastle upon Tyne: 727-745.

Boudin M., Van Strydonck M., Crombé P., De Clercq W., Van Dierendonck R., Jongepier H., Ervynck A. & Lentacker A., 2010. Fish reservoir effect on charred food residue ^{14}C dates: Are stable isotope analyses the solution? *Radiocarbon*, 52(2): 697-705. https://doi.org/10.1017/S0033822200045719

Boudin M., Van Strydonck M., Van den Brande T., Synal H.-A., Wacker L., 2015. RICH – A new AMS facility at the Royal Institute for Cultural Heritage, Brussels, Belgium. *Nuclear Instruments and Methods in Physics Research Section B: Beam Interactions with Materials and Atoms*, 361: 120-123.

Boudin M., Bonafini M., Van den Brande T., Van Strydonck M., 2016-2018 (2019). AGE: a new graphitisation apparatus for the ^{14}C-dating laboratory. *Bulletin KIK-IRPA*, 35/2016-2018, Bruxelles-Brussel: 197-201.

Bronk Ramsey C., 2009. Bayesian analysis of radiocarbon dates. *Radiocarbon*, 51(1): 337-360. https://doi.org//doi:10.1017/S0033822200033865

Bush R. T. & McInerney F. A., 2013. Leaf wax *n*-alkane distributions in and across modern plants: Implications for paleoecology and chemotaxonomy. *Geochimica et Cosmochimica Acta*, 117: 161-179. https://doi.org/10.1016/j.gca.2013.04.016

Casanova E., Knowles T. D. J., Bayliss A., Walton-Doyle C., Barclay A. & Evershed R. P., 2022. Compound-specific radiocarbon dating of lipid residues in pottery vessels: A new approach for detecting the exploitation of marine resources. *Journal of Archaeological Science*, 137: 105528. https://doi.org/10.1016/j.jas.2021.105528

Copley M. S., Berstan R., Dudd S. N., Docherty G., Mukherjee A. J., Straker V., Payne S. & Evershed R. P., 2003. Direct chemical evidence for widespread dairying in prehistoric Britain. *Proceedings of the National Academy of Sciences USA*, 100(4): 1524-1529. https://doi.org/10.1073/pnas.0335955100

Copley M. S., Hansel F. A., Sadr K. & Evershed R. P., 2004. Organic residue evidence for the processing of marine animal products in pottery vessels from the pre-colonial archaeological site of Kasteelberg D east, South Africa: research article. *South African Journal of Science*, 100(5): 279-283. https://hdl.handle.net/10520/EJC96255

Correa-Ascencio M. & Evershed R. P., 2014. High throughput screening of organic residues in archaeological potsherds using direct acidified methanol extraction. *Analytical Methods*, 6: 1330-1340. https://doi.org/10.1039/C3AY41678J

COUREL B., ROBSON H.K., LUCQUIN A., DOLBUNOVA E., ORAS E., ADAMCZAK K., ANDERSEN S. H., ASTRUP P. M., CHARNIAUSKI M., CZEKAJ-ZASTAWNY A., EZEPENKO I., HARTZ S., KABACIŃSKI J., KOTULA A., KUKAWKA S., LOZE I., MAZURKEVICH A., PIEZONKA H., PILIČIAUSKAS G., SØRENSEN S. A., TALBOT H. M., TKACHOU A., TKACHOVA M., WAWRUSIEWICZ A., MEADOWS J., HERON C. P. & CRAIG O. E., 2020. Organic residue analysis shows subregional patterns in the use of pottery by northern European hunter–gatherers. *Royal Society Open Science*, 7: 192016. https://doi.org/10.1098/rsos.192016

CRAIG O. E., 2004. Organic analysis of food crusts from sites in the Schelde valley, Belgium: a preliminary evaluation. *Notae Praehistoricae*, 24/2004: 209-217.

CRAIG O. E., 2021. Prehistoric Fermentation, Delayed-Return Economies, and the Adoption of Pottery Technology. *Current Anthropology*, 62 (suppl. 24): S233-S241. https://doi.org/10.1086/716610

CRAIG O. E., FORSTER M., ANDERSEN H., KOCH E., CROMBÉ P., MILNER N. J., STERN B., BAILEY G. N. & HERON C. P., 2007. Molecular and isotopic demonstration of the processing of aquatic products in northern European prehistoric pottery. *Archaeometry*, 49(1): 135-152. https://doi.org/10.1111/j.1475-4754.2007.00292.x

CRAIG O. E., ALLEN R. B., THOMPSON A., STEVENS R. E., STEELE V. J. & HERON C. P., 2012. Distinguishing wild ruminant lipids by gas chromatography/combustion/isotope ratio mass spectrometry. *Rapid Communications in Mass Spectrometry*, 26(19): 2359-2364. https://doi.org/10.1002/rcm.6349

CRAIG O. E., SAUL H. & SPITERI C., 2020. Residue analysis. In: Richards M. & Britton K. (ed.), *Archaeological Science: an introduction*. Cambridge University Press, Cambridge: 70-98. doi:https://doi.org/10.1017/9781139013826.004

CRAMP L. J. E. & EVERSHED R. P., 2014. Reconstructing aquatic resource exploitation in human prehistory using lipid biomarkers and stable isotopes. In: Holland H. D. & Turekian K. K. (ed.), *Treatise on Geochemistry: Archaeology and Anthropology (Second Edition)*, Elsevier, Amsterdam: 319-339. https://doi.org/10.1016/B978-0-08-095975-7.01225-0

CROMBÉ P., 2005. *The last hunter-gatherer-fishermen in Sandy Flanders (NW Belgium): the Verrebroek and Doel excavation projects*. Academia press, Ghent.

CROMBÉ P., 2010. Swifterbant pottery from the lower Scheldt Basin (NW Belgium). In: Vanmontfort B., Louwe Kooijmans L. P., Amkreutz L. & Verhart L. (ed.), *Pots, Farmers and Foragers: Pottery traditions and social interaction in the earliest Neolithic of the Lower Rhine Area*, Leiden University Press, Leiden: 161-165.

CROMBÉ P., VAN STRYDONCK M. & HENDRIX V., 1999. AMS-dating of antler mattocks from the Schelde river in northern Belgium. *Notae Praehistoricae*, 19/1999: 111-119.

CROMBÉ P., SERGANT J., PERDAEN Y., MEYLEMANS E. & DEFORCE K., 2015a. Neolithic pottery finds at the wetland site of Bazel-Kruibeke (Flanders, Belgium): evidence of long-distance forager-farmer contact during the late 6th and 5th millennium cal BC in the Rhine-Meuse-Scheldt area. *Archaologisches Korrespondenzblatt*, 45(1): 21-39.

CROMBÉ P., VERHEGGE J., DEFORCE K., MEYLEMANS E. & ROBINSON E., 2015b. Wetland landscape dynamics, Swifterbant land use systems, and the Mesolithic–Neolithic transition in the southern North Sea basin. *Quaternary International*, 378: 119-133.

CROMBÉ P., DE REU J., SERGANT J., BOUDIN M. & BOURGEOIS I., 2018. Prehistoric antler and bone tools from the Scheldt basin: new radiocarbon dates from the site of Wintam "Sluis" in the Rupel floodplain (municipality of Bornem, prov. of Antwerp, BE). *Notae Praehistoricae*, 38/2018: 15-26.

CRUZ F. & ROZEK J., 2023. *Antwerpen Scheldetunnel Linkeroever – Antwerpen, provincie Antwerpen, A600*. Nota, verslag van de resultaten van het landschappelijk bodemonderzoek, intern verslag GATE bvba, Sint-Michiels-Brugge.

DEFORCE K., 2014. *Middle Holocene vegetation and woodland exploitation of the lower Scheldt valley*. Doctoral dissertation, Ghent University, Ghent: 192 p.

DEFORCE K., STORME A., BASTIAENS J., DEBRUYNE S., DENYS L., ERVYNCK A., MEYLEMANS E., STIEPERAERE H., VAN NEER W. & CROMBÉ P., 2014. Middle-Holocene alluvial forests and associated fluvial environments: a multi-proxy reconstruction from the lower Scheldt, N Belgium. *Holocene*, 24(11): 1550-1564.

DEMIRCI Ö., 2022. Regional variation in the use of the earliest pottery in North-western Europe: organic residue analysis of Swifterbant pottery (5000-4000 cal. BC). Doctoral thesis, University of Groningen, Groningen: 215 p.

DEMIRCI Ö., LUCQUIN A., CRAIG O. E. & RAEMAEKERS D. C. M., 2020. First lipid residue analysis of Early Neolithic pottery from Swifterbant (the Netherlands, ca. 4300–4000 BC). *Archaeological and Anthropological Sciences*, 12: 105. https://doi.org/10.1007/s12520-020-01062-w

DUNNE J., 2022. Gone to seed? Early pottery and plant processing in Holocene north Africa. *Quaternary International*, 608/609: 178-193. https://doi.org/10.1016/j.quaint.2021.02.004

Evershed R. P., Mottram H. R., Dudd S. N., Charters S., Stott A. W., Lawrence G. J., Gibson A. M., Conner A., Blinkhorn P. W. & Reeves V., 1997. New Criteria for the Identification of Animal Fats Preserved in Archaeological Pottery. *Natur & Wissenschaften*, 84: 402-406. https://doi.org/10.1007/s001140050417

Fontes A. M., Geris R., dos Santos A. V., Pereira M. G., Ramalho J. G. S., da Silva A. F. & Malta M., 2014. Bio-inspired gold microtubes based on the morphology of filamentous fungi. *Biomaterial Science*, 2: 956-960. https://doi.org/10.1039/C4BM00030G

Gomart L., 2014. *Traditions techniques et production céramique au néolithique ancien : étude de huit sites rubanés du nord-est de la France et de Belgique*. Sidestone Press, Leiden: 342 p.

Hansel F. A., Copley M. S., Madureira L. A. S. & Evershed R. P., 2004. Thermally produced *ω*-(*o*-alkylphenyl) alkanoic acids provide evidence for the processing of marine products in archaeological pottery vessels. *Tetrahedron Letters*, 45(14): 2999-3002. https://doi.org/10.1016/j.tetlet.2004.01.111

Hillbrand M., Hadorn P., Cugny C., Hasenfratz A., Galop D. & Haas, J. N. 2012. The palaeoecological value of Diporotheca rhizophila ascospores (Diporothecaceae, Ascomycota) found in Holocene sediments from Lake Nussbaumersee, Switzerland. *Review of Palaeobotany and Palynology*, 186: 62-68. https://doi.org/10.1016/j.revpalbo.2012.06.009

Hurt V., 1982. Les haches en bois de cerf en Belgique : essai de classification. *Bulletin du Club Archéologique Amphora*, 29 : 14-24.

Kubo A. M., Gorup L. F., Amaral L. S., Filho E. R. & Camargo E. R., 2016. Kinetic Control of Microtubule Morphology Obtained by Assembling Gold Nanoparticles on Living Fungal Biotemplates. *Bioconjugate Chemistry*, 27(10): 2337-2345. https://doi.org/10.1021/acs.bioconjchem.6b00340

Livingstone Smith A., 2001. *Chaîne opératoire de la poterie. Références ethnographiques, analyses et reconstitution*. Thèse de doctorat, Université Libre de Bruxelles, Bruxelles: 462 p. Ibidem, [2001] 2007. *Idem*. Musée royal de l'Afrique centrale, Tervuren, 'Publications digitales': www.africamuseum.be > poterie.pdf

Louwe Kooijmans L. P., Oversteegen J. F. S. & van Gijn A. L., 2001. Artefacten van been, gewei en tand. In: Louwe Kooijmans L. P. (red.), *Archeologie in de Betuweroute: Hardinxveld-Giessendam Polderweg. Een mesolithisch jachtkamp in het rivierengebied (5500-500 v. Chr.)*, Rijksdienst voor het Oudheidkundig Bodemonderzoek, Rapportages Archeologische Monumentenzorg, 83, Amersfoort: 285-324.

Messiaen L., Vandendriessche H. & Crombé P., 2022. The Neolithization Process in the Lower-Scheldt Basin (Belgium, mid-6th to mid-4th Millennium cal BC) from a Lithic Technological Perspective. *Lithic Technology*, 48(2): 168-193. https://doi.org/10.1080/01977261.2022.2109354

Meylemans E., Perdaen Y., Sergant J., Bastiaens J., Crombé P., Debruyne S., Deforce K., Du Rang E., Ervynck A., Lentacker A., Storme A. & Van Neer W., 2016. *Archeologische opgraving van een midden-mesolithische tot midden-neolithische vindplaats te 'Bazel-Sluis 5' (gemeente Kruibeke, provincie Oost-Vlaanderen)*. Onderzoeksrapport agentschap Onroerend Erfgoed, 40, Brussel: 210 p. https://biblio.ugent.be/publication/01HGNQB6KCF7X8BQFSF4MSGYPT

Moore P. D., Webb J. A. & Collinson M. E., 1991. *Textbook of pollen analysis*. Blackwell, Oxford.

Papakosta V., Smittenberg R. H., Gibbs K., Jordan P. & Isaksson S., 2015. Extraction and derivatization of absorbed lipid residues from very small and very old samples of ceramic potsherds for molecular analysis by gas chromatography–mass spectrometry (GC–MS) and single compound stable carbon isotope analysis by gas chromatography–combustion–isotope ratio mass spectrometry (GC–C–IRMS). *Microchemical Journal*, 123: 196-200. https://doi.org/10.1016/j.microc.2015.06.013

Reimer P. J., Austin W. E. N., Bard E., Bayliss A., Blackwell P. G., Bronk Ramsey C., Butzin M., Cheng H., Edwards R. L., Friedrich M., Grootes P. M., Guilderson T. P., Hajdas I., Heaton T. J., Hogg A. G., Hughen K. A., Kromer B., Manning S. W., Muscheler R., Palmer J. G., Pearson C., van der Plicht J., Reimer R. W., Richards D. A., Scott E. M., Southon J. R., Turney C. S. M., Wacker L., Adolphi F., Büntgen U., Capano M., Fahrni S. M., Fogtmann-Schulz A., Friedrich R., Köhler P., Kudsk S., Miyake F., Olsen J., Reinig F., Sakamoto M., Sookdeo A. & Talamo S., 2020. The IntCal20 Northern Hemisphere Radiocarbon Age Calibration Curve (0–55 cal kBP). *Radiocarbon*, 62(4): 725-757. https://doi.org/doi:10.1017/RDC.2020.41

Regert M., 2011. Analytical strategies for discriminating archaeological fatty substances from animal origin. *Mass Spectrometry Reviews*, 30(2): 177-220. https://doi.org/10.1002/mas.20271

Romanus K., Poblome J., Verbeke K., Luypaerts A., Jacobs P., De Vos D. & Waelkens M., 2007. An evaluation of analytical and interpretative methodologies for the extraction and identification of lipids associated with pottery sherds from the site of Sagalassos, Turkey. *Archaeometry*, 49(4): 729-747. https://doi.org/10.1111/j.1475-4754.2007.00332.x

Shumilovskikh L. S., Schlütz F., Achterberg I., Bauerochse A. & Leuschner H. H., 2015. Non-pollen palynomorphs from mid-Holocene peat of the raised bog Borsteler Moor (Lower Saxony, Germany). *Studia Quaternaria*, 32(1): 5-18.

STEELE V. J., STERN B. & STOTT A. W., 2010. Olive oil or lard? Distinguishing plant oils from animal fats in the archaeological record of the eastern Mediterranean using gas chromatography/combustion/isotope ratio mass spectrometry. *Rapid Communications in Mass Spectrometry*, 24(23): 3478-3484. https://doi.org/10.1002/rcm.4790

STORME A., BASTIAENS J., CROMBÉ P., CRUZ F., LOUWYE S., VERHEGGE J. & DEFORCE K., 2020. The significance of palaeoecological indicators in reconstructing estuarine environments: A multi-proxy study of increased Middle Holocene tidal influence in the lower Scheldt river, N-Belgium. *Quaternary Science Reviews*, 230: 106113. https://doi.org/10.1016/j.quascirev.2019.106113

TEETAERT D., 2020. *Routes of technology: pottery production and mobility during the Mesolithic-Neolithic transition in the Scheldt river valley (Belgium)*. Doctoral thesis, Ghent University, Ghent: XXVIII-454 p.

TEETAERT D. & CROMBÉ P., 2022 [2023]. The prehistoric pottery from Melsele Hof ten Damme (East Flanders, BE). *Notae Praehistoricae*, 42/2022: 83-102.

TEETAERT D., BOUDIN M., SAVERWYNS S. & CROMBÉ P., 2017. Food and soot: organic residues on outer pottery surfaces. *Radiocarbon*, 59(5): 1609-1621. https://doi.org//10.1017/RDC.2017.25

TEETAERT D., BOUDIN M., GOEMAERE E., CROMBÉ P., 2020. Reliability of AMS 14C dates of moss temper preserved in Neolithic pottery from the Scheldt river valley (Belgium). *Radiocarbon*, 62(6): 1667-1678. https://doi.org/10.1017/RDC.2019.148

TEETAERT D., VANNOORENBERGHE M., VAN DE VELDE T., BOUDIN M., BODÉ S., KUBIAK-MARTENS L., BAERT M., LYNEN F., CROMBÉ P. & BOECKX P., 2024. Pottery use across the Neolithic transition in northern Belgium: evidence from isotopic, molecular and microscopic analysis. *Archaeological and Anthropological Sciences*, 16: 131. https://doi.org/10.1007/s12520-024-02030-4

VAN BERG P.-L., KEELEY L. H., VAN ROEYEN J.-P., VAN HOVE R., 1992. Le gisement mésolithique de Melsele (Flandre-Orientale, Belgique) et le subnéolithique en Europe occidentale. In: Le Roux C.-T. (ed.), *Paysans et bâtisseur. L'émergence du néolithique atlantique et les origines du mégalithisme. Actes du 17ᵉ Colloque interrégional sur le néolithique, Vannes, 28-31 octobre 1990*, (*Revue Archéologique de l'Ouest*, supplément 5), Rennes: 93-99.

VAN DER WIEL A. M., 1982. A palaeoecological study of a section from the foot of the Hazendonk (Zuid-Holland, The Netherlands), based on the analysis of pollen, spores and macroscopic plant remains. *Review of Palaeobotany and Palynology*, 38: 35-90. https://doi.org/10.1016/0034-6667(82)90049-5

VANSWEEVELT J., 2020. *Archeologienota Oosterweelverbinding Antwerpen. Resultaten van het vooronderzoek*. Nota van de stad Antwerpen, dienst archeologie, Antwerpen.

WOJCIESZAK M., VAN DEN BRANDE T., LIGOVICH G. & BOUDIN M., 2020. Pretreatment protocols performed at the Royal Institute for Cultural Heritage (RICH) prior to AMS ¹⁴C measurements. *Radiocarbon*, 62(5): 1-11. https://doi.org/10.1017/RDC.2020.64

Abstract

Recent excavations conducted in the framework of the Oosterweel Link infrastructure project (Antwerp, BE) have uncovered a small yet significant assemblage of prehistoric artefacts at site A600 Scheldetunnel Linkeroever. The finds include handmade pottery and antler artefacts, recovered from the interface between the basal peat horizon and the underlying Pleistocene sands. Based on the typo-technological characteristics of these artefacts and the available radiocarbon dates, they are interpreted as evidence of one or several nearby Swifterbant Culture occupations, dating to the middle to third quarter of the 5th millennium BCE. This timeframe is broadly contemporary with the earliest Swifterbant occupations at Doel Deurganckdok. These discoveries further underscore the potential for locating sealed Swifterbant sites within the Lower Scheldt area, for instance in the context of future expansions of the Port of Antwerp.

Keywords: Linkeroever (Antwerp, BE), A600 Scheldetunnel Linkeroever, Swifterbant Culture, pottery, antler mattocks, SEM, GC-MS, GC-C-IRMS, palynological analysis, radiocarbon dates.

Samenvatting

Recent archeologisch onderzoek in het kader van de aanleg van de Oosterweelverbinding (Antwerpen, BE) bracht een klein assemblage prehistorische artefacten aan het licht op de site A600 Scheldetunnel Linkeroever. Op de contactzone tussen het Pleistocene zand en de bovenliggende veenlaag werden een kleine hoeveelheid handgevormd aardewerk en twee artefacten in hertengewei aangetroffen. Op basis van de typo-technologische kenmerken van deze artefacten en de beschikbare ^{14}C-dateringen lijkt het te gaan om restanten van een of meerdere nabijgelegen occupaties van de Swifterbantcultuur, te dateren in het midden tot 3de kwart van het 5de millennium BCE. Dit toont nogmaals aan dat er een groot potentieel is voor het vinden van afgedekte Swifterbantsites in de Beneden-Scheldevallei, bijvoorbeeld in de context van toekomstige uitbreidingen van de haven van Antwerpen.

Kernwoorden: Linkeroever (Antwerpen, BE), A600 Scheldetunnel Linkeroever, Swifterbantcultuur, aardewerk, artefacten in hertengewei, SEM, GC-MS, GC-C-IRMS, pollenonderzoek, koolstofdateringen.

Dimitri Teetaert
Elliot Van Maldegem
Koen Deforce
Coralie André
Philippe Crombé
Universiteit Gent
Vakgroep Archeologie
Sint-Pietersnieuwstraat, 35
BE-9000 Gent
dimitri.teetaert@ugent.be
elliot.vanmaldegem@ugent.be
koen.deforce@ugent.be
coralie.andre@ugent.be
philippe.crombe@ugent.be

Daan Celis
Lies Dierckx
Veerle Hendriks
Femke Martens
Stad Antwerpen, Stadsontwikkeling
Onroerend Erfgoed
Francis Wellesplein, 1
BE-2018 Antwerpen
daan.celis@antwerpen.be
lies.dierckx@antwerpen.be
veerle.hendriks@antwerpen.be
femke.martens@antwerpen.be

Frédéric Cruz
Ruben Willaert NV
Ten Briele, 14
BE-8200 Sint-Michiels-Brugge
frederic.cruz@rubenwillaert.be

Samuel Bodé
Universiteit Gent
Vakgroep Groene Chemie en Technologie
Isotope bioscience laboratory (ISOFYS)
Coupure Links, 653
BE-9000 Gent
samuel.bode@ugent.be

Lucy Kubiak-Martens
Biologische archeologie & Landschapsreconstructie
BIAX Consult
Symon Spiersweg, 7-2D
NL-1506 RZ Zaandam
kubiak@biax.nl

Table des matières - Inhaltsverzeichnis - Inhoudstafel